

Original Research Article

Development of a Solar Power Generating System with Auto-Tracking and Data Logging Devices

ABSTRACT

Solar power systems have become a viable wellspring of sustainable energy over the years and are commonly used for a variety of industrial and domestic applications. Capturing and storing the maximum amount of available energy for prediction and future analysis have been the major problems. This study aimed at developing a solar power generating system with solar tracking and data logging devices. The Dual Axes Solar Power Generating System (DASPGS) was developed using a combination of hardware and software systems consisting of three major subsystems: mechanical, electro-mechanical, and electrical tracker parts. C-language programme was used in conjunction with the Arduino Uno board for logging the power generated from the DASPGS and already fabricated Fixed Axis Solar Power Generating System (FASPGS). The power generated was stored on the created web page and the Secure Digital (SD) card. Data were harvested and the performance evaluations of the DASPGS over FASPGS were determined for 28 days. DASPGS gave average power of 22.88, 22.25, 24.49, and 25.92 Watts per week while FASPGS gave 5.16, 15.00, 16.23, and 15.74 Watts per week. A significant difference between DASPGS and FASPGS gave a P value of .004. This study showed that the DASPGS performed better than FASPGS. The system developed finds its application in the area of solar power prediction.

Keywords: Data analysis, Data logging, Solar power system, Solar tracking system

1. INTRODUCTION

The increasing demand for energy and continuous depletion of fossil fuels coupled with the growing concern regarding environmental pollution have spurred researchers' interest in the exploration of safe, affordable, sustainable, clean, and green alternative energies like solar, wind, biomass, and hydropower energy. However, energy generation showed a major problem as the world population is increasing [1] and its demand is strongly driven by the needs of the growing population [2], thus, a typical sustainable energy source is needed. Solar energy source offers a huge prospect for the generation of electric power, capable of ensuring a significant quantum of electrical energy requirements for the planet earth [3]. This alternate source of power is constantly achieving admirable fame especially since the discovery of fossil fuel limitations for sustainable energy has generated much research interest in many countries of the world in line with the Sustainable Development Goal [4].

Acknowledging that solar energy is clean, renewable, and green/domestic energy source [5,6] available on daily bases from the sun and as such, it guaranteed a continuous supply of energy, especially in the daytime when the night times surplus energy from the supplies during the day can be stored up for use during hours of the night

34 through solar inverter system. However, there are situations when sufficient sunlight is not achieved during the day
 35 due to rainfall, storm, or cloudy or dull weather. Meteorologists have established that weather conditions are
 36 stochastic hence the need to engage in solar energy harvesting and storage using solar inverter systems. This
 37 study came up with a developed dual-axis solar power generator which was designed to capture energy from the
 38 sunlight by following the direction of sunlight at each time of the day.

39
 40 A solar tracking system enhances the optimum capturing of energy from sunlight as the solar panel was designed to
 41 follow the direction of direct sunlight throughout the day. This was considered to have the capacity to perform
 42 efficiently and effectively compared with the traditional fixed-position solar system. The major difference between
 43 the tracking system and the fixed-position solar system is the introduction of a solar mechanism that moves the set
 44 of connected solar cells on a dual axis along the path perpendicular to the ray of the sun [7,8]. Since the position of
 45 the sun keeps changing relative to the earth and to receive the best angle of exposure to sunlight for the collection
 46 of energy, a tracking mechanism is incorporated into the solar panel system to keep the panel pointed in the
 47 direction of the sun for optimum performance of the system [9].

48
 49 Azimuth and zenith have been identified as the most effective solar power tracker available due to their two-axis
 50 tracking movement [10]. Compared to the common properly fixed position solar panel, energy gain can be
 51 considerably increased using this type of solar tracking system [11]. These systems of tracking with two axes have
 52 been developed using two types of the most commonly used automatic control systems, open-loop, and closed-
 53 loop. Tracking in a closed-loop is more effective as it uses various active sensors responsible for receiving signals
 54 of solar radiation, such as Light Dependent Resistor (LDR) and it has feedback to the controller that allows constant
 55 orienting of the panel making the most of its effectiveness [12].

57 2. MATERIAL AND METHODS

58 2.1 Design of the DASP GS

59 The mechanical engineering material selection that was used for the fabrication and production of the DASP GS
 60 included the following: mild steel rod, mild steel pipe, mild steel bar, mild steel plate, galvanized steel pipe, chrome
 61 steel, aluminum pipe, carbon steel, and teflon. In the design of a gear drive, the following data were design
 62 parameters used: the power to be transmitted, the speed of the driving gear, the speed of the driven gear or the
 63 velocity ratio, and the center distance.

64 The gear ratio (G) 4:1 was used since the same material was used for the gear and pinion then, the design was
 65 based on the pinion since it is the weakest. The number of teeth on the pinion (T_p) was determined by equation 1.

$$66 T_p = \frac{2A_w}{G \left[\sqrt{1 + \frac{1}{G} \left(\frac{1}{G} + 2 \right) \sin^2 \varphi} - 1 \right]} \quad 1$$

67 where

68 T_G is number of teeth on the gear

69 D_p is pitch circle diameter of the pinion = 50mm

70 D_g is the pitch circle diameter of the gear = 200mm

71 A_w is fraction by which the standard for the wheel should be multiplied, = 1
 72 module, φ is pressure angle. For light shock intermittent load, $\varphi = 20^\circ$.

73 G is Gear ratio, G is Gear ratio = $\frac{T_G}{T_P} = \frac{D_G}{D_P} = 4$

74 Therefore, from Equation 1, we have:

$$75 T_p = 16 \text{ teeth}$$

76 The number of the teeth on gear was determined by Equation 2

$$77 T_G = G \times T_p \quad 2$$

$$78 \therefore T_G = 64 \text{ teeth} = 4 \times 16 = 64 \text{ teeth}$$

79 The center distance (L) between the shafts was determined using Equation 3

$$80 L = \frac{D_p}{2} + \frac{D_g}{2}$$

$$81 = \frac{50}{2} + \frac{200}{2} = 125 \text{ mm} \quad 3$$

82 The pitch line velocity (v) was determined using Equation 4, where N_p is Number of teeth pinion, =55 mm

$$83 v = \frac{\pi D_p N_p}{60} \quad 4$$

$$84 = 140 \text{ mm/s}$$

85 Since the pitch line velocity (v) is less than 12.5 m/s, therefore the velocity factor (C_v) was determined using
 86 Equation 5

$$87 C_v = \frac{3}{3+v} \quad 5$$

89
$$= \frac{3}{3+140} = 0.02$$

90 For $14\frac{1}{2}$ the composite and full-depth involute system, the tooth form factor (y_p) was determined using Equation 6

91
$$y_p = 0.124 - \frac{0.684}{T_p}$$
 6

92
$$= 0.081$$

93 Module (m) was determined using Equation 7

94
$$m = \frac{D_p}{T_p}$$
 7

95
$$= 3\text{mm}$$

96 For light shock intermittent load. The service factor (C_s) = 1, Then, tangential tooth load (W_T) was determined using

97 Equation 8, where P is power transmitted in watts, = 120 watts

98
$$(W_T) = \frac{P}{v} \times C_s$$
 8

99
$$= 0.8571\text{ N}$$

100 Lewis equation was applied since both the pinion and the gear are made of the same material, then the pinion is

101 weaker. Therefore, the width (b) of the pinion was determined using Equation 9

102
$$W_T = \sigma_{op} \cdot C_v \cdot b \cdot \pi \cdot m \cdot y_p$$
 9

103 where, σ_{op} is allowable static stress of the material selected, $\sigma_{op} = 22.4\text{ MPa}$

104
$$\therefore b = 2.5 \approx 3\text{mm}$$

105 The circular pitch (P_C) for gears to mesh correctly was determined using Equation 10

106
$$(P_C) = \frac{\pi D}{T_p} = \pi m$$
 10

107
$$= 9.43$$

108 The dynamic tooth load (W_D) was determined using Equations 11 to 13

109
$$W_D = W_T + W_I$$
 11

110 where,
$$W_I = \frac{21v(b.C+W_T)}{21v + \sqrt{b.C+W_T}}$$
 12

111 and C is a deformation or dynamic factor in N/mm,
$$C = \frac{K.e}{\frac{1}{E_p} + \frac{1}{E_g}}$$
 13

112 $K = 0.111$ = the factor depending upon the form of the teeth. For 20° full depth involute system,

113 e is tooth error action in mm, for pitch line velocity up to 1.25 m/s , $e = 0.0925$,

114 $E_p = E_g$ is young's modulus for the material of the pinion and gear in N/mm^2 ,

115
$$\therefore E_p = E_g = 0.583\text{Gpa.}$$

116 From Equation 13

117
$$C = 2.99 \times 10^6\text{ N/mm}$$

118 From equation 12

119
$$W_I = 4.45 \times 10^6\text{ N}$$

120 Therefore, W_D from equation 11 become

121
$$W_D = 4.45 \times 10^6\text{ N}$$

122 The static tooth load (W_s) was determined by Equation 14

123
$$W_s = \sigma_e \cdot b \cdot \pi \cdot m \cdot y_p$$
 14

124 where, σ_e is flexural endurance limit.

125 The Brinell Hardness Number (BHN) for Teflon is 294.

126 At 294 BHN, $\sigma_e = 490\text{ MPa}$, and $\sigma_s = 721\text{ MPa}$

127
$$\therefore$$
 From Equation 14,

128
$$W_s = 490 \times 10^6 \times 3 \times 493 \times 0.081 = 1.12 \times 10^9\text{ N}$$

129 For safety against tooth breakage, $W_s > W_D$. Wear tooth load (W_w) was determined by Equations 15 to 17

130
$$W_s = D_p \cdot b \cdot Q \cdot K$$
 15

131 Where, Q is the ratio factor for external gear,

132
$$Q = \frac{2T_G}{T_G + T_p}$$
 16

133 and K is a load stress factor in $\text{N/mm}^2 = \frac{(\sigma_{es})^2 \sin\phi}{1.4} \left[\frac{1}{E_p} + \frac{1}{E_g} \right]$ 17

134 From Equations 16 and 17

135
$$Q = 1.6$$

136
$$K = 437\text{ MPa}$$

137 Therefore Equation 15 becomes

138
$$W_s = 1.05 \times 10^{11}\text{ N}$$

139 The factor of safety (F_s) was determined by Equation 18

140
$$F_s = \frac{\text{Ultimate stress}}{\text{Allowable stress}}$$
 18

141 ≈ 1

142 The speed of the motor (N_{ss}) and the power (P_{ss}) on the horizontal solid shaft was taken as 55 rpm and 120 Watts,
143 respectively. Then, the torque (T_{ss}) for the threaded horizontal solid shaft was determined by Equation 19 as

$$144 \quad T_{ss} = \frac{P_{ss} \times 60}{2\pi N_{ss}} \quad 19$$
$$145 \quad = \frac{120 \times 60}{2 \times 3.142 \times 55} = 20.83 \text{ Nm} = 20830 \text{ Nmm}$$

146 Determination of the strength of the solid shaft (d_{ss}) was calculated using Equation 20, where the shear stress of
147 the mild steel, $\tau_{ss} = 258 \text{ MPa}$

$$148 \quad T_{ss} = \frac{\pi}{16} \times \tau_{ss} \times d_{ss}^3 \quad 20$$

149 \therefore Using Equation 20, we have

$$150 \quad d_{ss} = 7.44 \text{ mm} \approx 8 \text{ mm}$$

151 For the horizontal shaft, it is safe to use 7.44 mm but 8 mm was used

152 The speed of the motor (N_{hs}) and the power (P_{hs}) on the vertical hollow shaft was taken as 45 rpm and 180 Watts,
153 respectively. Then, the torque (T_{hs}) for the vertical hollow shaft was determined using Equation 21 as

$$154 \quad T_{hs} = \frac{P_{hs} \times 60}{2\pi N_{hs}} \quad 21$$
$$155 \quad = 38.2 \text{ Nm} = 38200 \text{ Nmm}$$

156 The diameter ratio for the vertical hollow shaft, (K_{hs}) = 0.8 was used and the shear stress for galvanized steel,
157 $\tau_{hs} = 10 \text{ MPa}$ Then, the external diameter for the hollow shaft (d_o) was determined by Equation 22

$$158 \quad d_o = \left[\sqrt[3]{\frac{16T_{hs}}{\pi\tau_{hs}} \left(\frac{1}{1-K_{hs}^4} \right)} \right] \quad 22$$
$$159 \quad = 0.032 \text{ m} = 32 \text{ mm} \text{ but } 35 \text{ mm} \text{ was used}$$

160 The internal diameter (d_i) was determined by Equation 23

$$161 \quad d_i = K_{hs} \times d_o \quad 23$$
$$162 \quad = 28 \text{ mm} \text{ but } 30 \text{ mm} \text{ was used}$$

163 2.2 Determination of the appropriate direction and orientation of the solar panel

164 Four Light Dependent Resistors were used as sensors for sensing light intensity. These LDRs faced four
165 different directions which are east, west, south, and west. Each LDRs was used in a voltage divider network whose
166 output was then connected to the analog pins of the microcontroller. Each LDR was used as R1, R2 R3, and R4 in
167 the circuit which made the output from each network to be directly proportional to the intensity of light falling on it.
168 Since four outputs were used then, four analog input pins were used on the Arduino board. The command analog
169 read was used to read the input and the microcontroller was used in comparing values gotten from each input pin, it
170 was then used to decide the correct direction to face by giving the direction which input is the highest preference
171 over others. Also, another Two LDRs were used, the first one was placed at an angle 90° . This was useful when the
172 sun passes overhead while the second one was placed at an angle 45° for tilting the solar panel perpendicular to
173 the direction of the sunlight.

174 After the decision is taken by the microcontroller, the microcontroller sent a signal to the first stepper motor to
175 rotate it to the concluded direction and then sent another signal to the second stepper motor to tilt the panel to face
176 the right direction. The microcontroller continued comparing the inputs from the voltage divider networks, and it
177 would take the process of actuation as soon as it sees a need for it. Figure 1 showed the circuit diagram of the
178 voltage divider network and the actuators while Figure 2 showed the product of the DASPGS.

179 2.3 Data logging development

180 The inner board of the data logging components for the DASPGS comprises the following;

- 181 • Casing: This is where data logging components of the DASPGS were enclosed.
- 182 • Arduino nano: This is where the C-language programme was written for logging the power generated from the
183 system.
- 184 • Display Screen: this is a digital display unit that showed the level of current rating in ampere coming directly from
185 the solar panel at a time, and the rate at which the battery is charging in volts.
- 186 • Secure Digital Card Module: This was used for the data logger which received information of data from Arduino
187 nano with the help of written language programme.
- 188 • Current Sensor: This was used to sense the level of current received from the solar panel
- 189 • Step down: This was used to step down the 12 volts coming from the battery to the 5 volts needed such as the
190 Arduino board, current sensor, SD card module, etc.
- 191 • GSM Module: this was used for an internet connection to enable data to be sent from Arduino to the created
192 website.
- 193 • Clock Module: This was used to set and update the time at which the data were uploaded
- 194 • Voltage Divider: This was used to divide the level of voltage, then convert it from analog signal to digital form
- 195 • Connector: This was used to connect the wire from the battery terminal.
- 196 • Variable Resistor: It was used for contrast which serves as control of the brightness and darkness of the screen.

197 **2.4 Principle of the data logging development**

198 A current sensor was used to measure the amount of current harvested by the solar panel and the amount of
199 voltage supply was measured using a voltmeter. The amount of power harvested was derived by multiplying the two
200 together using Equation (24) below

201 $Power, P = I \times V$

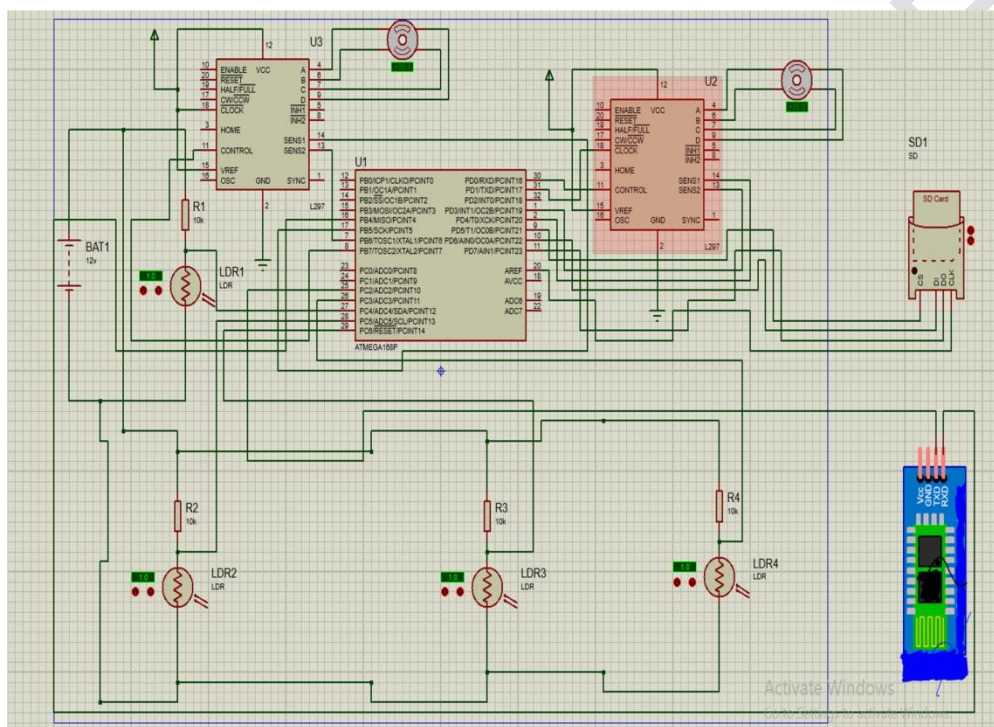
24

202 where I is current in amperes

203 V is voltage in volts

204 A computer programme was written in C-language in conjunction with the Arduino Uno board for logging the power
205 generated from the Dual Axis Solar Power Generating System (DASPGS) and Fixed Axis Solar Power Generating
206 System (FASPGS) at intervals of 5 minutes. The data were logged for both systems in two ways simultaneously.
207 For the first method, which is offline data logging, Secure Digital (SD) card and SD card module was used. This
208 module was connected to the microcontroller and the data was stored in it periodically in form of a comma-
209 separated value. The data stored were later retrieved by inserting the SD card in an SD card reader and then
210 opening the file stored in Microsoft (MS) excel.

211 For the online data logging, this was achieved by sending data to the server through the internet using a General
212 Packet Radio Service (GPRS) module. The data was received at the server side by a Hypertext Preprocessor
213 (PHP) script, which was then sent to the database. A web page was created using Hypertext Markup Language
214 (HTML) and PHP to fetch the data stored in the database and **display** it as web content. The full diagram of the
215 system is shown in Figure. 1 while Figure. 2 shows the system flow chart of the data logging.
216



217 **Fig. 1. The complete circuit diagram of the DASPGS**

218
219
220

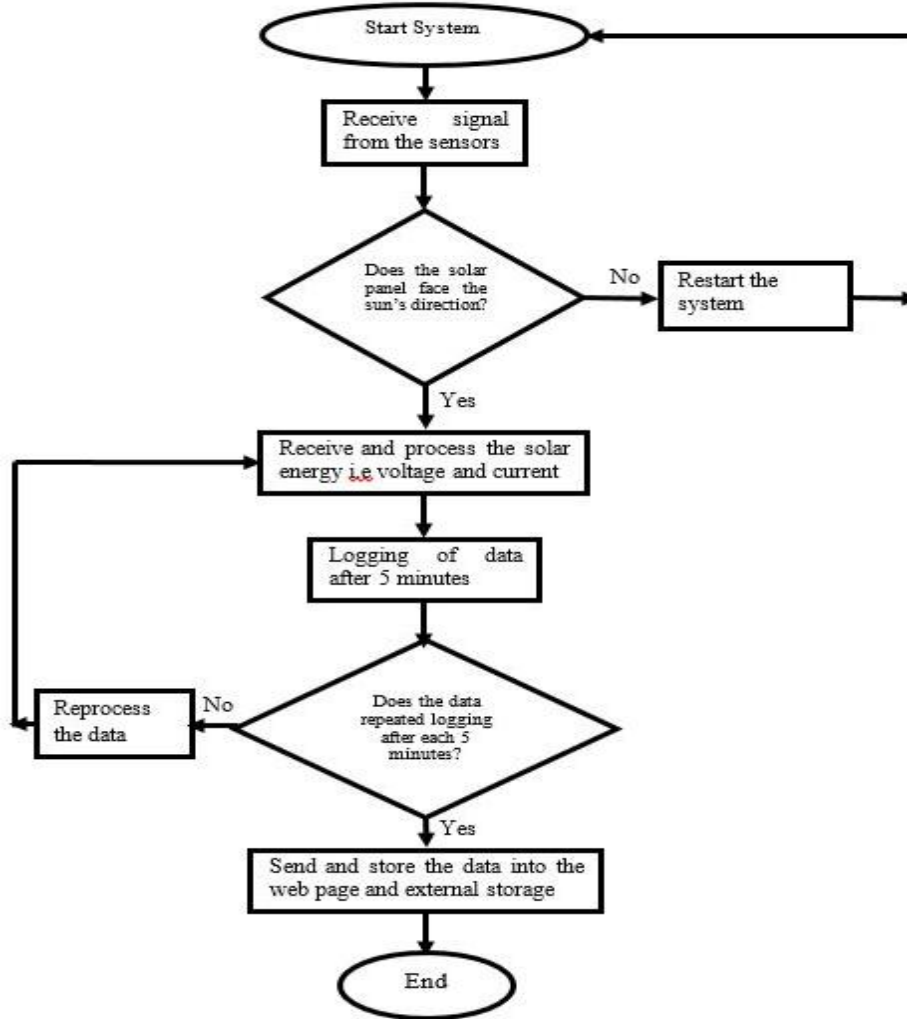


Fig. 2. Data Logging Flow Chart

221
222
223

2.5 Determination of the solar power system efficiency

The efficiency of the solar power system is the efficiency gained by using DASP GS over FASP GS and it was determined by Equation 25 according to [13].

$$\text{Efficiency gained} = \frac{D_a - F_a}{F_a} \times 100 \% \quad 25$$

where D_a is the power generated by DASP GS, and F_a is the power generated by FASP GS

2.6 Statistical analysis

Statistical Package for the Social Sciences (SPSS) version 23.0 using Analysis of Variance (ANOVA) was carried out to analyze the output power (data) collected from each of the DASP GS and the FASP GS. A significant difference in the daily data collected was determined to check whether there is a variation in the data points between DASP GS and FASP GS. Also, analyses were carried out to investigate if there are no significant differences between the data points on the days of the week that is Mondays, Tuesdays, Wednesdays, Thursdays, Fridays, Saturdays, and Sundays from each of the solar power systems. According to [14], the significant difference was determined by Equation 26 bellow

$$F = \frac{\sum n_j(\bar{x}_j - \bar{x})^2 / (k - 1)}{\sum \sum (x - \bar{x}_j)^2 / (N - k)} \quad 26$$

where F is the ANOVA coefficient,
 x is an individual observation
 \bar{x}_j is the sample mean of j^{th} treatment (or group),
 \bar{x} is the overall sample mean,
 k is the number of treatments of independent comparison,
 N is the total number of observations or total sample size

238
239
240
241
242
243

244
245
246
247
248

3. RESULTS AND DISCUSSION

3.1 Development of data logging devices

Figure 1 shows the developed DASPGS which rotates the solar panel along the direction of the sunlight while Figure 2 shows the data logging devices for recording and storing data.



Fig. 3. Dual Axis Solar Power Generating System

249
250
251

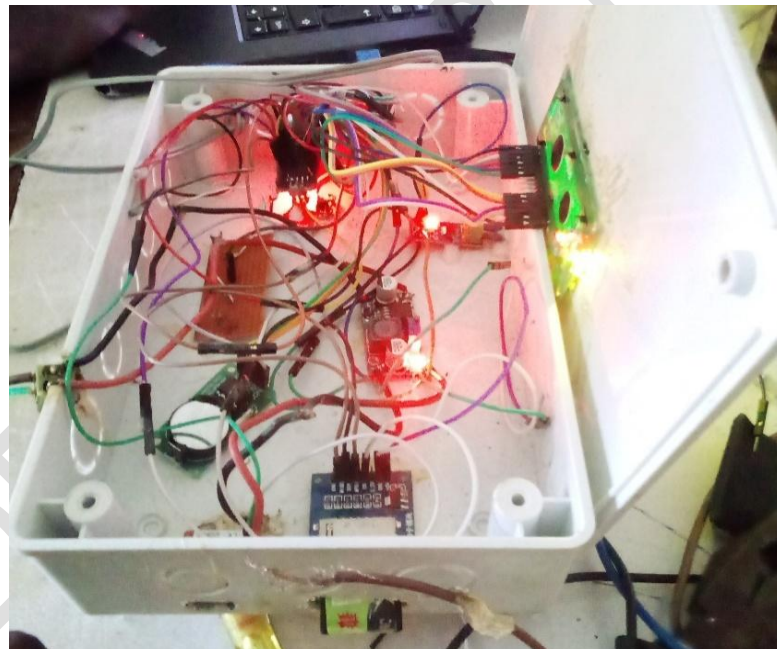


Fig. 4. Data logger devices

252
253
254
255
256
257
258
259
260
261
262
263
264
265

3.2 Average Power of the DASPGS and the FASPGS

The results of 2,016 data points (for current and voltage) were collected from the systems for four weeks between 10.00 AM to 4.00 PM daily at an interval of 5 minutes, thus the power for each data was determined. Figure 5 shows the relationship between the average power generated on daily basis for four weeks on the DASPGS and the FASPGS. The results showed that the DASPGS with tracking devices generated a maximum average power on the 28th day with 31.97 Watts while the minimum average power was obtained on the 16th day with 16.02 Watts. The FASPGS without tracking devices was able to generate a maximum average power per day on the 11th day with 19.76 Watts and the minimum average power was recorded on the 10th day with 9.65 Watts. However, after the days of experimentation, it was discovered that the daily average power values on DASPGS were always higher than the values of FASPGS which showed that the system developed was effective

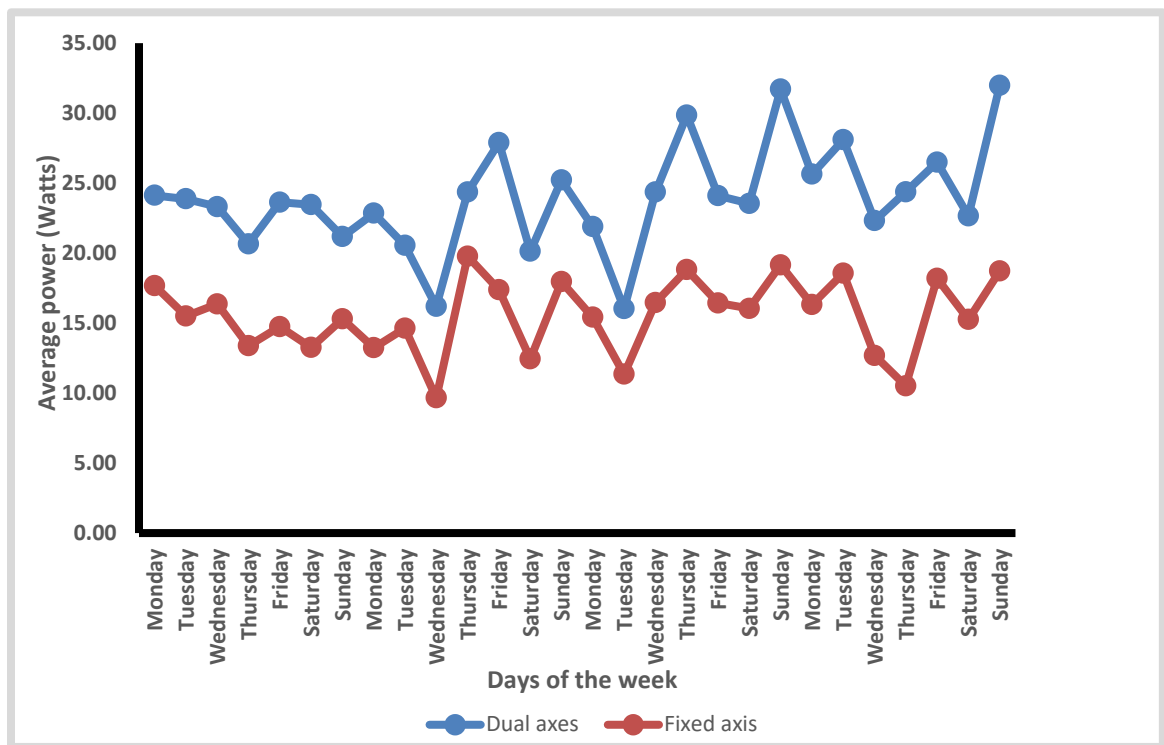


Fig. 5 Average power output per day

267
268
269
270
271
272
273
274
275
276
277
278
279
280
281

3.3 Performance evaluation of the system

The results of the performance evaluation of the DASP GS and FASP GS systems are shown in Table 1. The results showed that the values of the average power generated in the first week from the DASP GS and FASP GS systems were 22.88 and 15.16 Watts, respectively and the efficiency gain by the system developed (DASP GS) was 50.92%. Consequently, the values of the average power generated by DASP GS and FASP GS, and the efficiencies for the second, third, and fourth weeks were 22.45 Watts, 15.00 Watts, and 49.67%; 24.49 Watts, 16.23 Watts, and 50.89%; 25.92 Watts, 15.74 Watts, and 64.68%, respectively. However, research conducted by [15] stated that the efficiency of the DASP GS can be improved by 30-50% relative to FASP GS. Therefore, it was observed that the DASP GS was increased during the four weeks of testing of the system developed with an average efficiency gain of 54.04%.

Table 1. Efficiency of the data logging solar power system

Week	Average Power on		Efficiency Gained (%)
	DASP GS Solar System (Watt)	FASP GS Solar System (watt)	
1	22.88	15.16	50.92
2	22.45	15.00	49.67
3	24.49	16.23	50.89
4	25.92	15.74	64.68
Average Efficiency Gained =			54.04

282
283
284
285
286
287
288

3.4 Comparative analysis results

The Analysis of Variance (ANOVA) of the DASP GS and FASP GS, setting Hypothesis;
 H_0 = There are no significant differences between the set of data for DASP GS and FASP GS and the Alternative hypothesis;
 H_1 = There are significant differences between the set of data for DASP GS and FASP GS systems.

289 According to [16], explained to determine significant differences between the set of data, at a 95% confidence
290 level, if the P value is = .05 implies that there is a significant difference and if the P value is > .05 it means there is
291 no significant difference.
292

293 3.5 Comparison between DASP GS and FASP GS

294 Table 2 shows the results of the ANOVA test conducted on 2016 data points to check if there is a variation
295 between DASP GS and FASP GS. The standard deviations of 9.676 and 7.144 were obtained from DASP GS and
296 FASP GS respectively. These values are an indication of how the data points per 5 minutes are spread out from the
297 mean values of 23.930 and 15.488 respectively. Meanwhile, the variance of 93.632 and 51.045 agree with the
298 standard deviation which also informed how dispersed the data points are to the mean or average values. For all
299 the days in four weeks, the P value obtained is .004 which is less than 0.05 meaning that there is a significant
300 difference between the set of data on DASP GS and FASP GS.
301

302 **Table 2. ANOVA result for significant difference between DASP GS and DASP GS**

Test	DASP GS	FASP GS
Standard deviation	9.676	7.144
Average	23.930	15.488
Variance	93.632	51.045.
P value	.004	

303
304
305

306 3.6 ANOVA test for DASP GS and FASP GS on the day of the weeks

307 Table 3 shows the results of the test conducted using ANOVA to check if there is any significant or no
308 significant difference between the data collected from the DASP GS and the FASP GS on days of the four weeks. It
309 was observed that the P value indicated that there is a significant difference between the set of data in the DASP GS
310 on Mondays, Tuesdays, Wednesdays, Thursdays, and Sundays while there is no significant difference on
311 Saturdays of the four weeks. Whereas, It was observed that the P value indicated that there is a significant
312 difference between the set of data in the FASP GS on Mondays, Tuesdays, Wednesdays, and Saturdays while there
313 is no significant difference on Thursdays, Fridays, and Sundays of the four weeks.

Table 3 ANOVA results for DASP GS and FASP GS on the days of the weeks

4 Weeks	DASP GS P value	FASP GS P value
Mondays	.02	.002
Tuesdays	.01	.001
Wednesdays	.002	.001
Thursdays	.004	.58*
Fridays	.03	.26*
Saturdays	.06*	.02
Sundays	.006	.27*

314 * Note that the P values > .05
315

316 4. CONCLUSION

317 A data logging system was developed for DASP GS and FASP GS. Performance evaluation of the DASP GS
318 gave a 54.04% increase over FASP GS. A significant difference was observed through the ANOVA test conducted
319 on the power outputs between DASP GS and the FASP GS with a P value of .004 which is less than the .05
320 statistical index. No significant differences were observed on Saturdays for the DASP GS with a P value of .06,
321 while, FASP GS gave no significant difference on Thursdays, Fridays, and Sundays with P values of .58, .26, and
322 .27, respectively.
323

324 REFERENCES

325
326 1. Rabaia MKH, Abdelkareem MA, Sayed ET, Elsaid K, Chae KJ, Wilberforce T, Olabi AG. Environmental impacts
327 of solar energy systems: A review. Science of The Total Environment. 2021;754-989.
328
329

- 330 2. Mondal S, Mondal AK, Chintala V, Tauseef SM, Kumar S, Pandey JK. Thermochemical pyrolysis of biomass
331 using solar energy for efficient biofuel production: a review. *Biofuels*. 2021;12(2):125-134.
- 332 3. Wang J, Lu C. Design and Implementation of a Sun Tracker with a Dual-Axis Single Motor for an Optical Sensor-
333 Based Photovoltaic System. 2013;(13):3157-3168.
- 334 4. The Sustainable Development Goals Report. SDG; 2017.
- 335 5. Srinivasan M, Velu A, Madhubabu B. Potential Environmental Impacts of Solar Energy Technologies.
336 *International Journal of Science and Research*. 2019;8(5):792-795
- 337 6. Aman MM, Solangi KH, Hossain MS, Badarudin A, Jasmon GB, Mokhlis H, Kazi SN. A review of Safety, Health
338 and Environmental (SHE) issues of the solar energy system. *Renewable and Sustainable Energy*
339 *Reviews*. 2015;(41):1190-1204.
- 340 7. Otieno OR. Solar Tracker for Solar Panel. University of Nairobi; 2015.
- 341 8. Shekhawat RS, Rao RS, Kumari K, Kumar V. Solar Panel Using Inverter with Level Indicator. *International*
342 *Journal of Innovative and Emerging Research in Engineering*. 2016;3(3):77-83.
- 343 9. Ramya P, Ananth R. The Implementation of Solar Tracker Using Arduino With Servomotor. *International*
344 *Research Journal of Engineering and Technology*. 2016;3(8):969-72.
- 345 10. Morón C, Ferrández D, Saiz P, Vega G. New Prototype of Photovoltaic solar tracker based on arduino. *Energie*.
346 2017: Available from: www.mdpi.com/journal/energy
- 347 11. Jäger K, Isabella O, Arno HM, René ACM, Miro Z. Solar energy: Fundamentals, Technology, and Sytems.
348 *Green Energy and Technology*. Delft University of Technology. 2014:159-214.
- 349 12. Hong T, Jeong K, Ban C, Oh J, Koo C, Kim J, Lee M. A preliminary study on the two-axis hybrid solar tracking
350 method for the smart photovoltaic blind. *Energy Procedia*. 2016;88:484-490.
- 351 13. Deepthi S, Ponni A, Ranjitha R, Dhanabal R. Comparison of Efficiencies of Single-Axis Tracking System and
352 Dual-Axis Tracking System with Fixed Mount. *International Journal of Engineering Science and Innovative*
353 *Technology (IJESIT)*. 2013;2(2):425-430.
- 354 14. Ajayeoba AO, Fajobi MO, Raheem WA, Adebisi KA, Olayinka M. Risk Factor Assessments and Development of
355 Predictive Model for Volatile Organic Compounds Emission in Petrol Stations in Nigeria. *Digital Innovation and*
356 *Contemporary Research in Science, Engineering and technology*. 2021;9(1):57-74.
- 357 15. Johnson-Hoyte D, Rossi D, Johnson-Hoyte D, Rossi D. Dual-Axis Solar Tracker : Functional Model Realization
358 and Full-Scale Simulations. Faculty of Worcester Polytechnic Institute; 2013.
- 359 16. Onawumi AS, Dunmade IS, Ajayi OO, Sangotayo EO, Oderinde MO. The investigation into House-Hold Energy
360 Consumption in Saki, Southwestern Nigeria. *International Journal of Scientific and Engineering Research*.
361 2016;7(3):720-727.